minerals

Carrier Flotation Using Coarse Pyrite for Improving the Recovery of Finely Ground Chalcopyrite: Development of Post-Process of Carrier Flotation to Separate Finely Ground Chalcopyrite Particles from Coarse Pyrite Particles

Muhammad Bilal [1], Ilhwan Park [2,*], Mayumi Ito [2], Fawad Ul Hassan [1], Kosei Aikawa [2], Sanghee Jeon [3] and Naoki Hiroyoshi [2]

1   Department of Mining Engineering, Balochistan University of Information Technology, Engineering, and Management Sciences (BUITEMS), Quetta 87300, Pakistan; muhammad.bilal1@buitms.edu.pk (M.B.); fawad.hassan@buitms.edu.pk (F.U.H.)
2   Division of Sustainable Resources Engineering, Faculty of Engineering, Hokkaido University, Sapporo 060-8628, Japan; itomayu@eng.hokudai.ac.jp (M.I.); k-aikawa@eng.hokudai.ac.jp (K.A.); hiroyosi@eng.hokudai.ac.jp (N.H.)
3   Department of Earth Resource Engineering and Environmental Science, Faculty of International Resources Science, Akita University, Akita 010-0865, Japan; jeon@gipc.akita-u.ac.jp
*   Correspondence: i-park@eng.hokudai.ac.jp; Tel.: +81-11-706-6315

Abstract: Carrier flotation is a technique that can recover fine particles by using coarse carrier particles during the flotation process. In heterogeneous carrier flotation, coarse mineral particles of different minerals are used as carriers to recover fine mineral particles. By using Cu^{2+}-treated pyrite particles as carriers, fine chalcopyrite particles recovery could be improved. However, a disadvantage of this heterogeneous carrier flotation is that it requires a post-flotation separation process to improve the grade of the final Cu concentrate. This study tested mechanical and chemical treatments to detach finely ground chalcopyrite ($D_{50} \sim 3.5$ μm) particles from Cu^{2+}-treated coarse pyrite particles ($-125 + 106$ μm) after flotation. The results showed that the ultrasonic treatment was not effective to detach chalcopyrite fines from Cu^{2+}-treated pyrite particles. However, acid treatment was effective to detach chalcopyrite fines from coarse pyrite particles. At pH 2, approximately 96% of chalcopyrite fines were detached from coarse Cu^{2+}-treated pyrite particles. The acid treatment of flotation froth (mixture of chalcopyrite fines and Cu^{2+}-treated pyrite particles) decomposed the collector KAX (potassium amyl xanthate) and dissolved the Cu precipitates adsorbed on the pyrite surface. This weakened the hydrophobic attraction force between the chalcopyrite fines and coarse pyrite particles, thus promoting the detachment of chalcopyrite fines from Cu^{2+}-treated coarse pyrite particles.

Keywords: heterogeneous carrier flotation; fine particles; chalcopyrite; pyrite; hydrophobic interaction

1. Introduction

Flotation is a widely used mineral processing method for separating metal sulfides from gangue [1–9]. Before flotation, ore particles are ground to liberate gangue from ore. After grinding, the flotation process is carried out and hydrophobic (water-repellent) mineral particles are separated from hydrophilic (water-loving) gangue minerals [9–12]. When the particle size becomes too small, the flotation efficiency drops significantly [13]. Fine mineral particles are less likely to be recovered in flotation due to the low collision probability between fine particles and air bubbles [7,14–21]. Low-grade copper deposits will become increasingly important as high-grade ores are depleted. Typically, low-grade ores contain fine grains that require fine grinding in order to liberate the target minerals. Due to this, fine particles generation will pose a challenge to the mining industry, especially in mechanical flotation circuits that fail to operate efficiently with fine particles, resulting in

valuable minerals being lost in tailings. The development of an efficient flotation technique can make tailings the future deposits.

Carrier flotation is a promising method for improving the recovery of fine particles. The autogenous carrier flotation method uses the same mineral particles of coarse size to recover fine mineral particles. Using coarse chalcopyrite as a carrier (autogenous carrier flotation), the flotation recovery of finely ground chalcopyrite was significantly improved [11]. One of the advantages of autogenous carrier flotation is that it does not require a post-flotation process [1] and the Cu grade in the final concentrate is maximum. However, considering tailings as future deposits, this autogenous carrier flotation may have limited applicability because of the non-availability of coarse copper mineral particles at the tailings site. That is why an alternative carrier is required to recover fine copper sulfides from tailings.

Pyrite is a suitable choice as a carrier because of its abundance at mine sites. In previous research, the authors investigated the heterogeneous carrier flotation technique using coarse Cu^{2+}-treated pyrite as a carrier and demonstrated that by using coarse Cu^{2+}-treated pyrite particles as the carrier, the flotation recovery of finely ground chalcopyrite particles can be significantly improved [22]. Moreover, it was revealed that a hydrophobic interaction is the key factor in the attachment of fine chalcopyrite particles to coarse Cu^{2+}-treated pyrite particles [22].

Although effective, heterogeneous carrier flotation using Cu^{2+}-treated pyrite as a carrier has a drawback; that is, there is a low Cu grade in the concentrate because a significant amount of coarse pyrite particles is also contained together with fine chalcopyrite particles in the froth. In actual industrial mineral processing operations, a smelter requires a specific grade of copper. Therefore, in the case of heterogeneous carrier flotation using pyrite as a carrier, the development of the post-flotation process to separate attached fine copper minerals from carrier pyrite is needed to obtain a high-grade Cu concentrate.

This paper aims to develop the post-process of heterogeneous carrier flotation. In this study, two methods (i.e., ultrasonic treatment and acid treatment) were investigated to detach fine chalcopyrite from coarse pyrite (i.e., carrier) by reducing the hydrophobic interaction between them—a major force for these two particles to be attached. Specifically, the suitable conditions of these two methods for the detachment were examined, and the mechanisms of how fine chalcopyrite was detached from coarse pyrite were clarified.

2. Materials and Methods

2.1. Materials and Reagents

2.1.1. Materials

In this study, the same samples of chalcopyrite and pyrite were used as described in the previous article [22]. Pyrite and chalcopyrite samples were obtained from the Huanzala Mine (Huallanca, Peru) and the Copper Queen Mine (Bisbee, AZ, USA), respectively. Impurities were removed via handpicking after the samples were hammered. Mineralogical and chemical characterizations of pyrite and chalcopyrite were carried out using X-ray fluorescence (XRF) (EDXL300, Rigaku Corporation, Tokyo, Japan) and X-ray powder diffraction (XRD, Multiplex, Rigaku Corporation, Tokyo, Japan) techniques. The mineralogical and chemical compositions of these samples are shown in Figure 1 [22] and Table 1, respectively.

Table 1. Chemical compositions of chalcopyrite and pyrite samples used in this study.

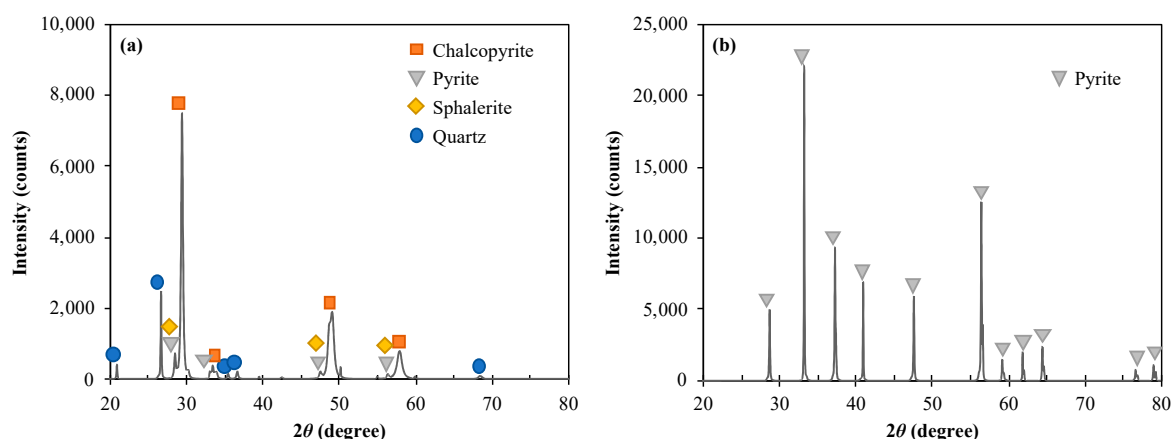| Minerals	Mass (%)						
	Cu	Fe	S	Zn	Si	Ca	Others
Chalcopyrite	30.0	32.0	18.0	0.6	5.0	4.0	10.4
Pyrite	0.05	45.3	48.5	-	1.0	-	5.15

Figure 1. XRD patterns of (**a**) chalcopyrite and (**b**) pyrite samples (reprinted with permission from Bilal et al. [22], copyright (2022) Elsevier).

2.1.2. Reagents

Potassium amyl xanthate (KAX, $C_5H_{11}OCSSK$) (Tokyo Chemical Industry Co., Ltd., Tokyo, Japan) and methyl isobutyl carbinol (MIBC, $C_6H_{14}O$) (Wako Pure Chemical Industries, Ltd., Osaka, Japan) were used as collector and frother, respectively. Copper sulfate pentahydrate ($CuSO_4 \cdot 5H_2O$) (Wako Pure Chemical Industries, Ltd., Japan) was used as the source of Cu^{2+} for pyrite activation. Dilute HCl and NaOH were used for changing the pH.

2.2. Methods

2.2.1. Sample Preparation

A jaw crusher (1023-A, Yoshida Manufacturing Co., Ltd., Sapporo, Japan) and disc mill (RS200, Retsch Inc., Haan, Germany) were used to crush and grind the samples, respectively. Fresh samples were prepared for each experiment to avoid the effect of oxidation. The particle size distributions of coarse pyrite ($D_{50} \sim 104$ μm) and fine chalcopyrite ($D_{50} \sim 3.5$ μm) determined using Microtrac (MT3300SX, Nikkiso Co., Ltd., Tokyo, Japan) are shown in Figure 2.
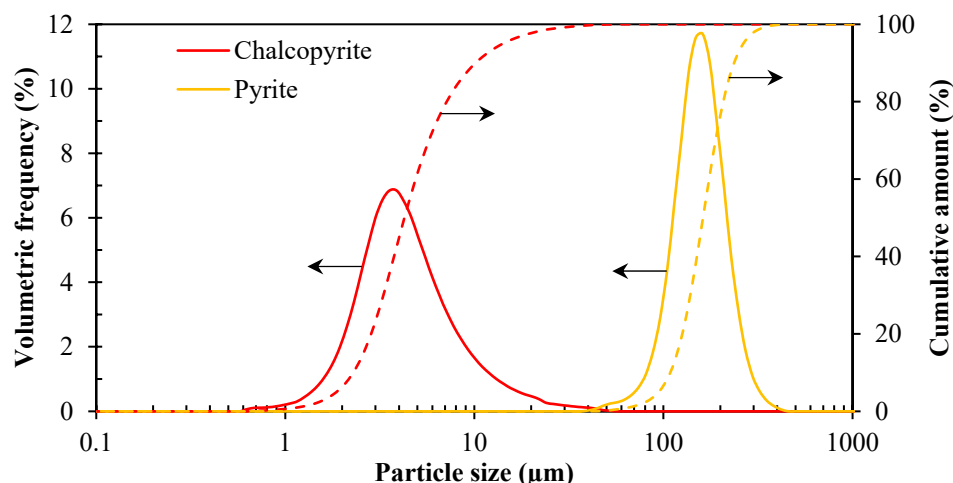

Figure 2. Particle size distributions of chalcopyrite and pyrite samples.

2.2.2. Mixed Chalcopyrite–Pyrite Flotation Tests

In total, 10 g of coarse pyrite particles and 20 g of fine chalcopyrite particles were sequentially conditioned with reagents $CuSO_4$ (2000 g/t) for 5 min, KAX (500 g/t) for 5 min, and MIBC (25 μL/L) for 3 min. The parameters were the same as those in the previous paper [22]. The pH of the slurry was 8 and it was kept constant during the conditioning. After the desired conditioning time, flotation was performed at an agitation

speed of 1000 rpm and air flow rate of 1 L/min for 10 min. The froth product was then analyzed using Microtrac to check the attachment of fines onto the carrier.

2.2.3. Detachment of Finely Ground Chalcopyrite from Coarse Pyrite
Ultrasonic Treatment

The froth product obtained after the mixed pyrite–chalcopyrite flotation test was put into a beaker, mixed with 200 mL distilled water, and then treated using an ultrasonicator (W-113, Honda Electronics Co., Ltd., Japan) at 31 Hz for up to 30 min. Afterward, a particle size analysis was conducted to verify the detachment of finely ground chalcopyrite from coarse pyrite.

Acid Treatment

Similar to the above subsection, a 200 mL suspension was prepared by mixing the froth product and distilled water. The suspension pH was adjusted to 8 using dilute NaOH while stirring at 1000 rpm, and 1 mL aliquot was taken for particle size analysis. Afterward, the pH of the suspension was gradually decreased up to 2 using dilute HCl, and the changes in particle size distributions were measured.

2.2.4. XPS Analysis

The surfaces of Cu^{2+}-treated pyrite samples treated at different pH values were analyzed via X-ray photoelectron spectroscopy (XPS, JPS-9200, JEOL Ltd., Akishima, Japan) to verify whether the Cu compounds formed on the surface of pyrite remained after the acid treatment. The residue was then collected from the suspension via filtration, dried for 24 h at 40 °C in a vacuum oven, and then analyzed. The XPS analysis was performed using an Al Kα X-ray source (1486.7 eV) operated at 100 W (voltage = 10 kV; current = 10 mA) under ultra-high vacuum conditions (~6.7×10^{-7} Pa). The C 1 s (285 eV) was used as a reference for charge correction in order to calibrate the photoelectrons' binding energies. The XPS data were analyzed using Casa XPS, and the spectra were deconvoluted using an 80% Gaussian–20% Lorentzian peak model and a true Shirley background [23–26].

2.2.5. FTIR Analysis

The Cu^{2+}-treated pyrite samples treated at different pH values were analyzed via attenuated total reflectance Fourier transform infrared spectroscopy (ATR-FTIR, FT/IR-6200 HFV, and ATR Pro One attachment equipped with a diamond prism, Jasco Analytical Instruments, Japan) to verify whether the KAX was decomposed or not. Cu^{2+}-treated pyrite was conditioned with KAX at different pH values for 20 min, each in the flotation cell at 1000 rpm. Afterward, the residue was recovered from the suspension via filtration, dried in a vacuum oven at 40 °C for 24 h, and analyzed via ATR-FTIR.

2.2.6. Dissolution Test of Cu^{2+} from Cu^{2+}-Activated Pyrite

A total of 10 g of pyrite sample was mixed with 400 mL DI water at 1000 rpm, and the suspension pH was adjusted to pH 8. After this, pyrite was conditioned with 2000 g/t $CuSO_4$ for 5 min followed by 500 g/t KAX for 5 min, and the leachate was then collected via filtration using a 0.2 μm syringe-driven membrane filter and immediately analyzed using an inductively coupled plasma atomic emission spectrometer (ICP-AES, ICPE 9820, Shimadzu Corporation, Japan) (margin of error = ±2%) to measure the concentration of Cu^{2+}. Similarly, the pH of the suspension was gradually decreased up to 2 using dilute HCl, and the samples were taken and analyzed for the concentration of Cu^{2+} dissolved from Cu^{2+}-activated pyrite.

3. Results and Discussion
3.1. Heterogeneous Carrier Flotation of Fine Chalcopyrite Using Coarse Pyrite as a Carrier

In a previous study conducted by the authors [22], heterogenous carrier flotation of fine chalcopyrite using coarse pyrite as a carrier was studied. As shown in Figure 3,

Cu recovery without the addition of carrier was ~70% but slightly decreased to 63% when the carrier was added, indicating that fine chalcopyrite was not attached onto the surface of pyrite. The addition of pyrite rather adversely affected Cu recovery due to the reduction in KAX adsorbed on the surface of chalcopyrite. To improve the attachment of fine chalcopyrite to coarse pyrite, the authors investigated the effect of the activation of pyrite by Cu^{2+} on the heterogeneous carrier flotation of fine chalcopyrite. After the activation of pyrite by Cu^{2+}, its surface was covered with Cu_2S and $CuO/Cu(OH)_2$ compounds that improved the hydrophobic interaction between fine chalcopyrite and Cu^{2+}-activated pyrite by ~6 times compared to that between fine chalcopyrite and untreated pyrite. Cu recovery via heterogeneous carrier flotation using Cu^{2+}-activated pyrite was improved to >90%, indicating that the addition of Cu^{2+}-activated pyrite particles as carriers is promising for improving the recovery of fine chalcopyrite via flotation. However, as mentioned in the Introduction, the purity of Cu concentrates obtained via heterogeneous carrier flotation is low due to the presence of a large amount of pyrite. In the next section, the post-process of heterogeneous carrier flotation for improving the purity of Cu concentrates by separating fine chalcopyrite and coarse pyrite will be discussed.
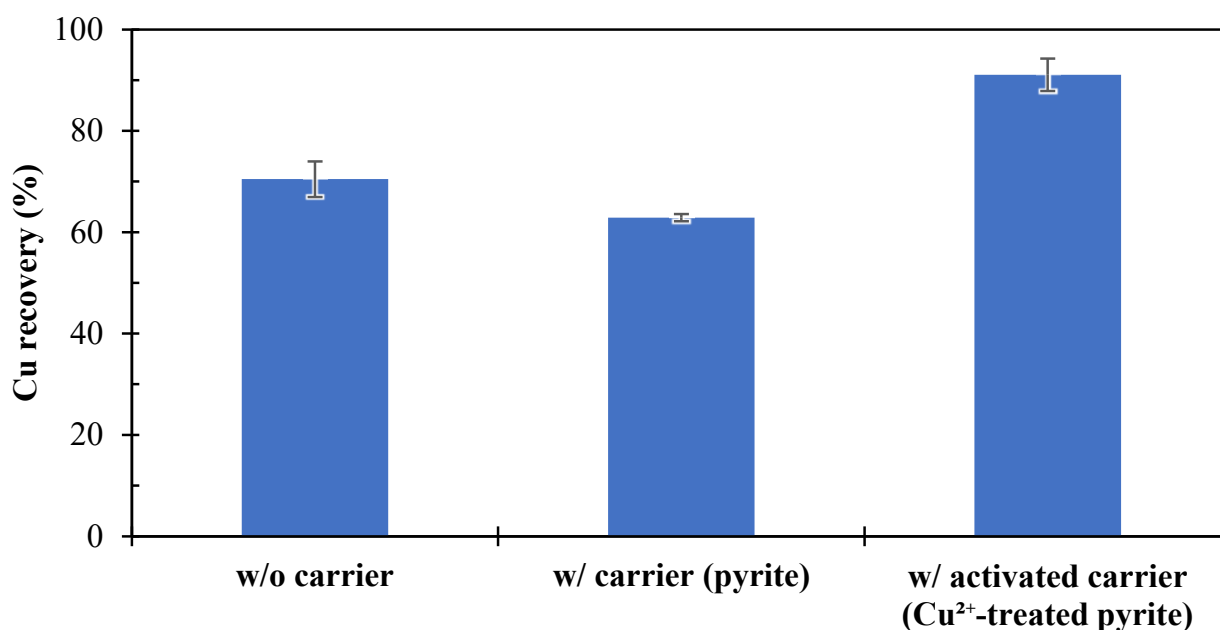

Figure 3. Cu recovery from fines with and without coarse pyrite (untreated and activated by Cu^{2+}) as a carrier. Test conditions: [KAX], 500 g/t; [MIBC], 25 μL/L; [$CuSO_4$], 2000 g/t; carrier size, −125 + 106 μm; carrier amount, 10 g (reprinted with permission from Bilal et al. [22], copyright (2022) Elsevier).

3.2. Ultrasonic Treatment on the Detachment of Chalcopyrite from Cu^{2+}-Treated Pyrite

A carrier flotation experiment for 20 g of fine chalcopyrite was conducted using 10 g of coarse Cu^{2+}-treated pyrite particles as the carrier with xanthate as the collector. The froth product was suspended in 200 mL of distilled water and agitated; then, ultrasonic treatment was applied for 30 min.

Figure 4 shows the particle size distribution of the suspended froth product before the ultrasonic treatment. The dotted line is reference data calculated from the amount of chalcopyrite and pyrite in the froth by assuming that there is no attachment of chalcopyrite fines to coarse pyrite particles. In the reference data, there are two peaks corresponding to fine chalcopyrite at approximately 3.5 μm and coarse pyrite at approximately 150 μm. In the size distribution curve for the suspended froth product, the peak located at approximately 3.5 μm was very small, indicating that most of the fine chalcopyrite particles in the froth were attached to coarse Cu^{2+}-treated pyrite particles. Moreover, the peak at approximately

150 μm was shifted to approximately 250 μm, indicating that fine particles were attached to the surface of coarse pyrite particles, and that the coarse–coarse particles agglomerates were formed.
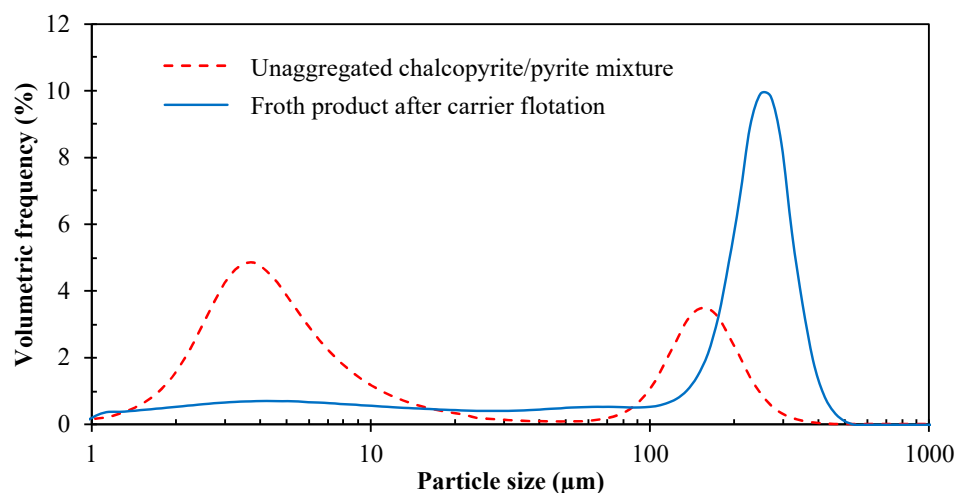

Figure 4. Particle size distribution of the froth product of fine chalcopyrite and coarse pyrite particles before ultrasonic treatment (measured vs. calculated).

Figure 5 shows the effects of ultra-sonication on the particle size distribution for the suspended froth product. The curve indicated with "0 min (before ultrasonic treatment)" is the same as the solid blue line shown in Figure 4. If fine chalcopyrite particles are detached from coarse pyrite particles, there would be an increase in the peak at 3.5 μm. The observed data, however, show that there was no significant increase in the peak at 3.5 μm after 30 min of ultrasonic treatment. This suggests that the ultrasonic treatment is not effective in detaching chalcopyrite fines from Cu^{2+}-treated pyrite particles.
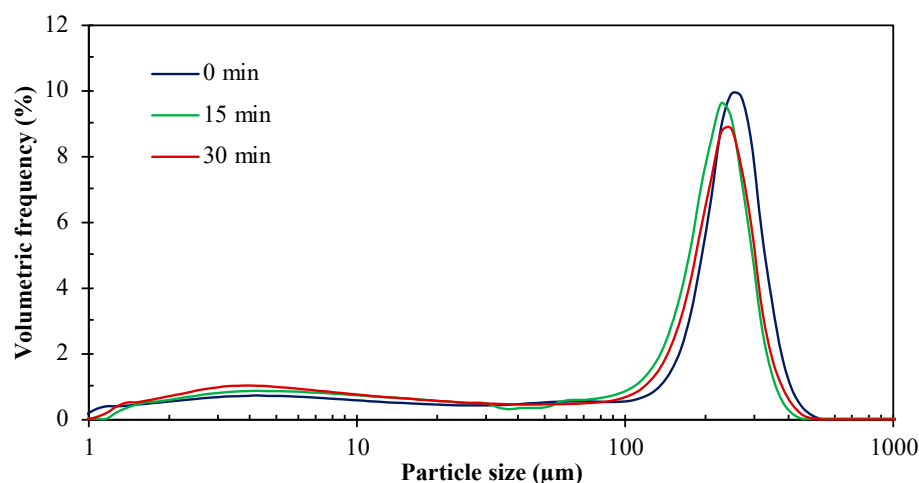

Figure 5. Particle size distribution of the froth product of fine chalcopyrite and coarse pyrite particles at different intervals of ultrasonic treatment time.

In our previous research, it was found that the hydrophobic interaction is the main reason for the attachment of fine chalcopyrite to coarse Cu^{2+}-treated pyrite: the potential energy of hydrophobic interaction between fine chalcopyrite and coarse Cu^{2+}-treated pyrite was evaluated to be approximately -200×10^{-18} J when the distance between two particle surfaces is 10 nm [22]. As shown in Figure 5, the ultrasonic treatment could not detach chalcopyrite fines from Cu^{2+}-treated coarse pyrite particles, which indicates two possibilities: (1) the intensity of ultrasonic treatment is not enough to overcome the

hydrophobic interaction; and (2) the detachment occurs but the particles become re-attached due to hydrophobic interactions. This suggests that rather than supplying the kinetic energy, a reduction in the hydrophobic interaction is needed. In the next section, this approach is discussed.

3.3. Acid Treatment on the Detachment of Chalcopyrite from Cu^{2+}-Treated Pyrite

The hydrophobic interaction between chalcopyrite and Cu^{2+}-treated pyrite is mainly caused by (1) the CuO/CuS layer formed on the pyrite surface, and (2) the collector (KAX) adsorbed on both chalcopyrite and the CuO/CuS layer. It has been reported that at low pH (<4), the collector (KAX) adsorbed onto the surface of the particle could be decomposed [27]. It is also possible that the CuO layer can also be decomposed (or dissolved) in acidic solutions.

Considering the above, the acid treatment was applied to reduce the hydrophobic interaction between chalcopyrite and Cu^{2+}-treated pyrite. HCl was added to the suspension of the flotation froth product to adjust the pH to ~2. Figure 6 shows the effect of acid treatment on the particle size distribution of the suspended flotation froth product. After 20 min of acid treatment, a significant peak corresponding to fine chalcopyrite (at approximately 3.5 μm) was observed. The peak at approximately 250 μm before the treatment was shifted to approximately 200 μm after the acid treatment. This may be due to both the detachment of chalcopyrite from pyrite and the decomposition of pyrite–pyrite agglomerates. This result suggests that the acid treatment is effective in reducing the hydrophobic interaction and causes the detachment of fine chalcopyrite from coarse Cu^{2+}-treated pyrite.
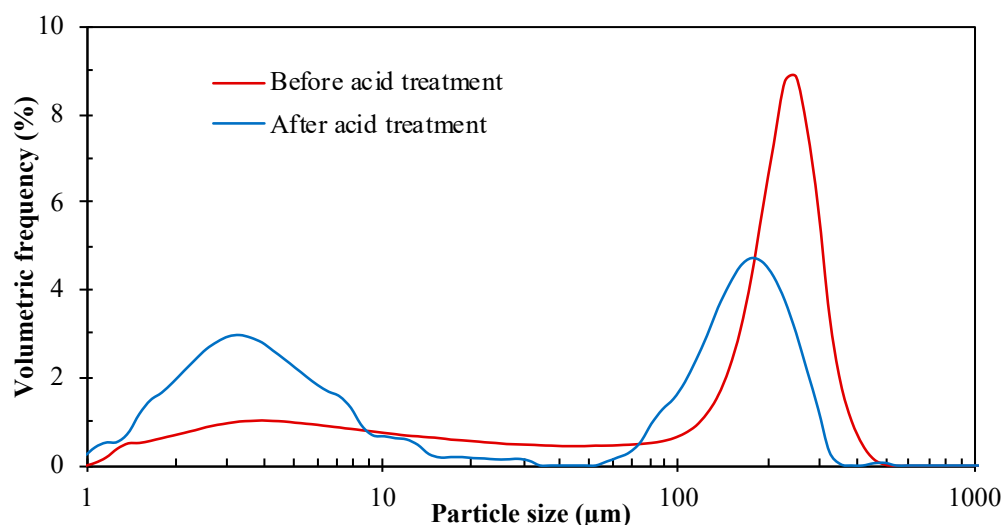

Figure 6. Particle size distribution of the froth product of fine chalcopyrite and coarse pyrite particles before and after acid treatment.

To optimize the pH condition for the acid treatment, the particle size distributions for the mixture of 20 g of fine chalcopyrite particles and 10 g coarse Cu^{2+}-treated pyrite particles suspended in a 400 mL flotation cell after conditioning with KAX at pH 8 and then changing the pH to 5, 4, 3 and 2 were analyzed using Microtrac. For comparison, a calculated size distribution curve for the mixture was obtained, assuming no attachment of chalcopyrite fines to coarse pyrite particles, and a comparison has been devised with the measured data (Figure 7). From Figure 8, it can be seen that at pH 8, approximately 38% of fines were attached to coarse Cu^{2+}-treated pyrite particles. However, the detachment of fines from coarse Cu^{2+}-treated pyrite particles increased with a decrease in pH. The detachment of fines was not significant at pH 4–8 but it was effective at pH < 4, i.e., at pH 2, the cumulative frequency of fines was approximately 97%, suggesting that hydrophobic interactions between coarse and fine particles became weaker. As mentioned earlier, the reduction in the hydrophobic interaction mostly results from the dissolution

of Cu compounds present on the surface of Cu^{2+}-treated pyrite and/or the decomposition of KAX adsorbed on mineral surfaces, which will be clarified in more detail in the following subsections.
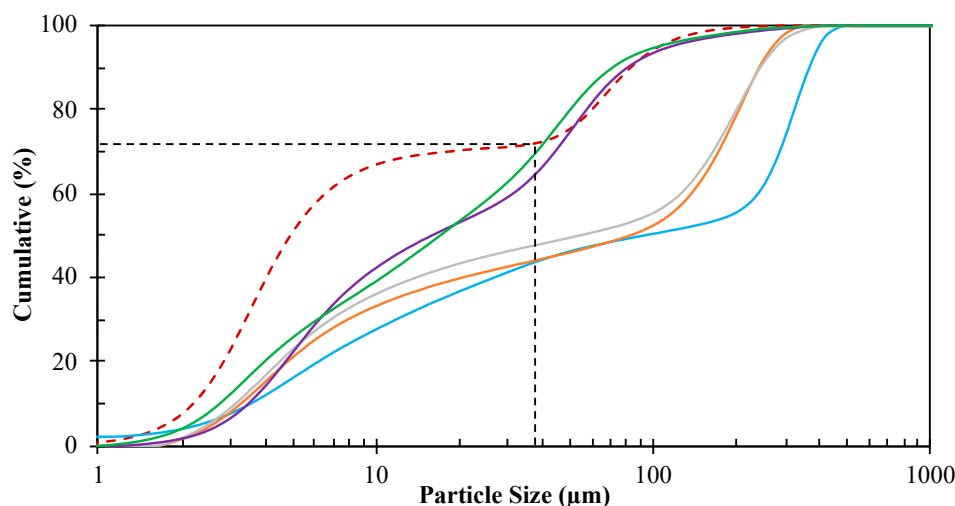
Figure 7. Particle size distribution of the mixture of fine chalcopyrite and coarse Cu^{2+}-treated pyrite particles after conditioning (measured vs. calculated).
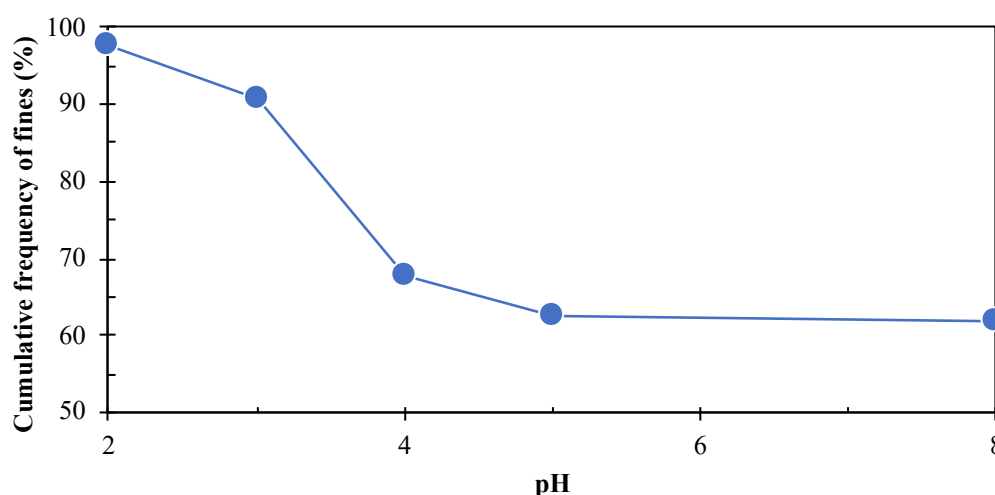
Figure 8. Measured cumulative amount of chalcopyrite fines at different pH values.

3.3.1. Dissolution of Cu Compounds Formed on the Surface of Cu^{2+}-Treated Pyrite at Different pH Values

Dissolution tests of Cu compounds formed on the surface of Cu^{2+}-treated pyrite at different pH values were conducted. As shown in Figure 9, almost all of Cu^{2+} was precipitated when the pH was approximately 8. However, it can be seen that when the pH was decreased, the dissolution of Cu^{2+} increased significantly, i.e., ~95% at pH 2.

After the dissolution tests, the residues were analyzed via XPS to verify the changes in the intensities of Cu species present on the surface of pyrite. Figure 10 shows the Cu 2p spectra of Cu^{2+}-treated pyrite at different pH values. In the Cu $2p_{3/2}$ spectrum of Cu^{2+}-treated pyrite at pH 8 (Figure 10i), there is a strong peak at ~932 eV corresponding to Cu_2S [28], as well as minor peaks at approximately 933.4 eV and 934.9 eV that are both assigned to Cu(II) species like $CuO/Cu(OH)_2$ [28,29]. However, the intensities of these peaks were reduced when Cu^{2+}-activated pyrite was treated at pH 4 (Figure 10ii), and it was further reduced at pH 2 (Figure 10iii), indicating that the Cu compounds adsorbed on pyrite surface have been dissolved.
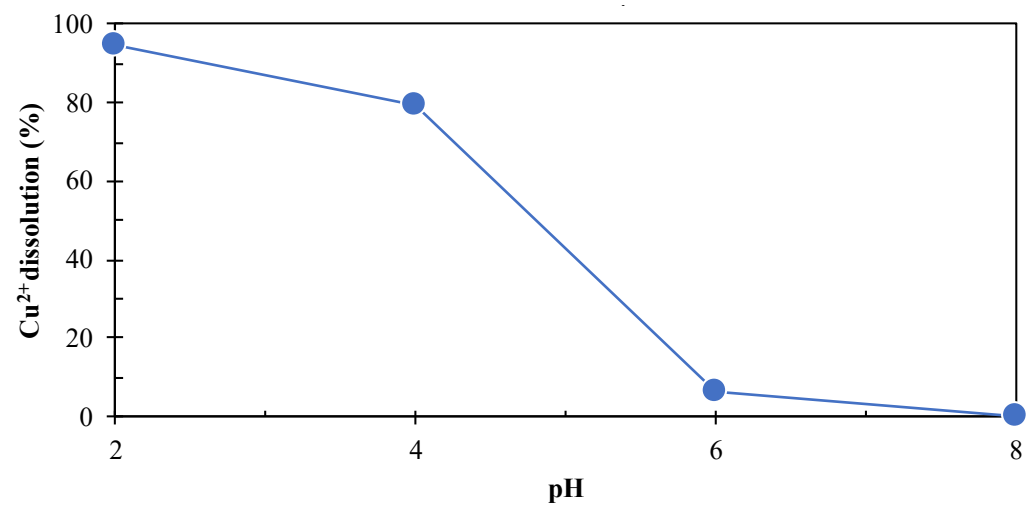
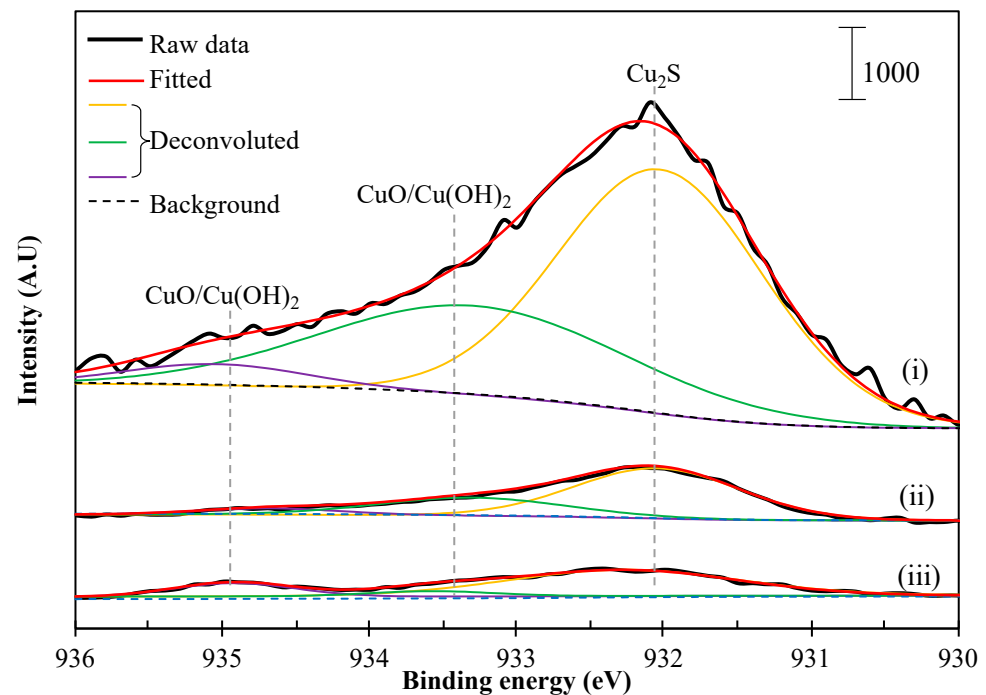**Figure 9.** Dissolved Cu concentration after dissolution test.

Figure 10. XPS Cu 2p3/2 spectra of Cu^{2+}-treated pyrite: (i) pH 8, (ii) pH 4, and (iii) pH 2.

Surface modification is an effective method of controlling mineral hydrophobicity [30–32]. The KAX adsorption on pyrite becomes easier when a CuS-like layer or its oxidized products, such as $Cu(OH)_2$, can be formed on the surface of pyrite [33]. Pyrite particles become more hydrophobic, making them better carriers for fine chalcopyrite particles during flotation. Due to the fact that acid treatment dissolves the CuO layer formed on the pyrite surface (Figures 9 and 10), the collector (KAX) adsorbed on the surface of Cu^{2+}-treated pyrite could be desorbed; therefore, chalcopyrite fines can be detached from coarse pyrite particles (Figures 7 and 8). Thus, the dissolution of Cu compounds formed on the surface of pyrite via acid treatment significantly contributes to the detachment of fine chalcopyrite and coarse pyrite.

3.3.2. Decomposition of KAX Adsorbed on the Surface of Pyrite

Both the formation of Cu compounds and the adsorption of KAX play an important role in improving the hydrophobic interaction between fine chalcopyrite and coarse pyrite.

Under acidic conditions, it is known that KAX is readily decomposed [27]; therefore, its decomposition was verified using an ATR-FTIR analysis of Cu^{2+}-activated pyrite treated at various pH values (2–8). As shown in Figure 11, the IR spectrum of Cu^{2+}-activated pyrite treated with KAX at pH 8 showed the absorption bands of the hydrophobic tail of KAX (e.g., asymmetric, and symmetric stretching bands of CH_3–CH_2 at 2977, 2927, 2887, and 2830 cm^{-1}) [7,34]. Moreover, Cu^{2+}-activated pyrite treated with KAX at pH 8 showed only the absorption bands of C–O–C, S–C–S, and C–O–S at 1116 cm^{-1}, 1084 cm^{-1} and 945 cm^{-1}, respectively [35,36]. The IR spectrum of Cu^{2+}-activated pyrite treated with KAX at pH 4 showed only a weak absorption band of S–C–S detected at 1084 cm^{-1}. Meanwhile, the IR signatures of KAX were not observed in the spectrum of Cu^{2+}-activated pyrite treated with KAX at pH 2, which indicates that KAX started being decomposed at pH 4, and it is completely decomposed at pH 2. This supports our earlier deduction that at low pH (~2), Cu precipitates could be dissolved and KAX could be decomposed, thereby reducing the hydrophobic attractive force between mineral particles and promoting detachment.
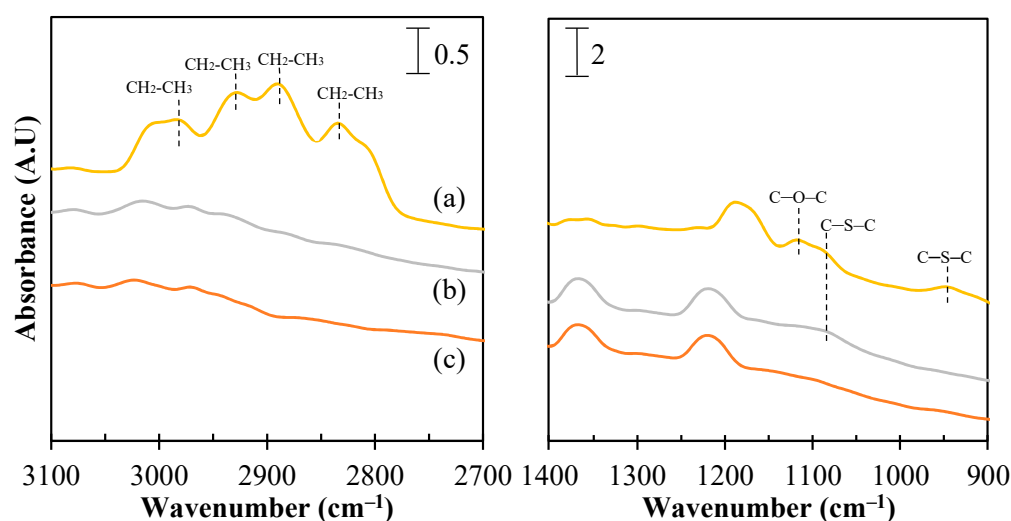

Figure 11. FTIR spectra of pyrite treated with KAX: (a) pH 8, (b) pH 4, and (c) pH 2.

3.4. Proposed Flowsheet for Heterogenous Carrier Flotation

To separate fine chalcopyrite particles from Cu^{2+}-treated pyrite particles after the acid treatment of the froth product of the heterogeneous carrier flotation (chalcopyrite fines and Cu^{2+}-treated coarse pyrite as the carrier), the suspension of the acid-treated froth product was poured onto the screen of 75 μm. The results showed that approximately 90% of the Cu in the froth was recovered as a passing product and it was separated from the retained product, which is mainly composed of coarse pyrite. Based on the results, a flow sheet was proposed to integrate the heterogenous carrier flotation into the existing flotation circuits in order to recover fine copper sulfides from low-grade deposits/tailings and reuse the coarse pyrite as a carrier (Figure 12). Tailings may contain fine pyrite particles, and, during copper activation, they may attach to coarse pyrite particles. To avoid this, it was proposed that coarse pyrite particles should be pre-treated with $CuSO_4$ separately, as this will allow only fine copper sulfides particles to attach to coarse treated pyrite particles and fine pyrite particles will not attach to coarse treated pyrite particles.
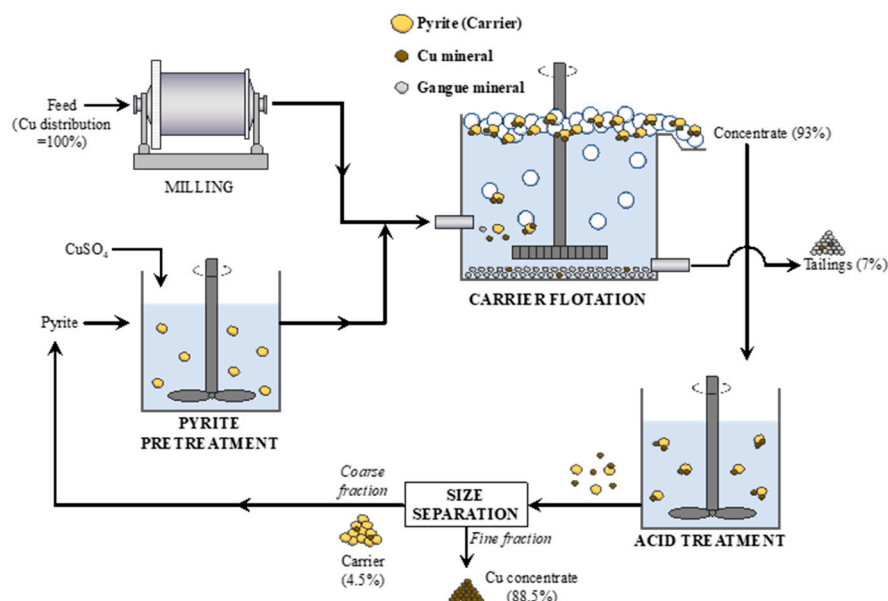
Figure 12. Proposed flowsheet of heterogeneous carrier flotation for low-grade deposits/tailings.

4. Conclusions

In this paper, the separation of finely ground chalcopyrite and coarse pyrite from froth products obtained after heterogeneous carrier flotation carried out using an ultrasonic treatment or acid treatment was investigated. Between the two methods, the acid treatment was only effective in detaching chalcopyrite fines from Cu^{2+}-treated coarse pyrite particles. Under the acidic conditions (pH~2), the hydrophobic interactions between chalcopyrite fines and Cu^{2+}-treated coarse pyrite particles were reduced due to the dissolution of Cu-compounds present on the surface of Cu^{2+}-treated pyrite as well as due to the decomposition of KAX adsorbed mineral surfaces. This suggests that after heterogeneous carrier flotation combined with acid treatment (post flotation), coarse pyrite may be reused as a carrier and the grade of final Cu concentrate could be improved.

Author Contributions: Conceptualization, M.B., I.P., M.I., S.J. and N.H.; methodology, M.B., K.A. and N.H.; investigation, M.B.; writing—original draft preparation, M.B. and I.P.; writing—review and editing, M.B., I.P., M.I., F.U.H., K.A., S.J. and N.H.; visualization, I.P.; supervision, M.I. and N.H. All authors have read and agreed to the published version of the manuscript.

References

1. Li, D.; Yin, W.; Liu, Q.; Cao, S.; Sun, Q.; Zhao, C.; Yao, J. Interactions between fine and coarse hematite particles in aqueous suspension and their implications for flotation. *Miner. Eng.* **2017**, *114*, 74–81. [CrossRef]
2. Bagster, D.F.; McIlvenny, J.D. Studies in the selective flocculation of hematite from gangue using high molecular weight polymers. Part 1: Chemical factors. *Int. J. Miner. Process.* **1985**, *14*, 1–20. [CrossRef]
3. Sivamohan, R. The problem of recovering very fine particles in mineral processing—A review. *Int. J. Miner. Process.* **1990**, *28*, 247–288. [CrossRef]
4. Song, S.; Lu, S. Hydrophobic Flocculation of Fine Hematite, Siderite, and Rhodochrosite Particles in Aqueous Solution. *J. Colloid Interface Sci.* **1994**, *166*, 35–42. [CrossRef]
5. Park, I.; Hong, S.; Jeon, S.; Ito, M.; Hiroyoshi, N. A Review of Recent Advances in Depression Techniques for Flotation Separation of Cu–Mo Sulfides in Porphyry Copper Deposits. *Metals* **2020**, *10*, 1269. [CrossRef]
6. Zhang, Q.; Niu, C.; Bu, X.; Bilal, M.; Ni, C.; Peng, Y. Enhancement of Flotation Performance of Oxidized Coal by the Mixture of Laurylamine Dipropylene Diamine and Kerosene. *Minerals* **2021**, *11*, 1271. [CrossRef]

7.	Hornn, V.; Park, I.; Ito, M.; Shimada, H.; Suto, T.; Tabelin, C.B.; Jeon, S.; Hiroyoshi, N. Agglomeration-flotation of finely ground chalcopyrite using surfactant-stabilized oil emulsions: Effects of co-existing minerals and ions. *Miner. Eng.* **2021**, *171*, 107076. [CrossRef]

8.	Aikawa, K.; Ito, M.; Segawa, T.; Jeon, S.; Park, I.; Tabelin, C.B.; Hiroyoshi, N. Depression of lead-activated sphalerite by pyrite via galvanic interactions: Implications to the selective flotation of complex sulfide ores. *Miner. Eng.* **2020**, *152*, 106367. [CrossRef]

9.	Wang, X.; Bu, X.; Alheshibri, M.; Bilal, M.; Zhou, S.; Ni, C.; Peng, Y.; Xie, G. Effect of scrubbing medium's particle size distribution and scrubbing time on scrubbing flotation performance and entrainment of microcrystalline graphite. *Int. J. Coal Prep. Util.* **2021**, *42*, 3032–3053. [CrossRef]

10.	Yin, W.; Xue, J.; Li, D.; Sun, Q.; Yao, J.; Huang, S. Flotation of heavily oxidized pyrite in the presence of fine digenite particles. *Miner. Eng.* **2018**, *115*, 142–149. [CrossRef]

11.	Bilal, M.; Ito, M.; Koike, K.; Hornn, V.; Ul Hassan, F.; Jeon, S.; Park, I.; Hiroyoshi, N. Effects of coarse chalcopyrite on flotation behavior of fine chalcopyrite. *Miner. Eng.* **2021**, *163*, 106776. [CrossRef]

12.	Zhou, S.; Bu, X.; Wang, X.; Ni, C.; Ma, G.; Sun, Y.; Xie, G.; Bilal, M.; Alheshibri, M.; Hassanzadeh, A.; et al. Effects of surface roughness on the hydrophilic particles-air bubble attachment. *J. Mater. Res. Technol.* **2022**, *18*, 3884–3893. [CrossRef]

13.	Trahar, W.J. A rational interpretation of the role of particle size in flotation. *Int. J. Miner. Process.* **1981**, *8*, 289–327. [CrossRef]

14.	Trahar, W.J.; Warren, L.J. The flotability of very fine particles—A review. *Int. J. Miner. Process.* **1976**, *3*, 103–131. [CrossRef]

15.	Miettinen, T.; Ralston, J.; Fornasiero, D. The limits of fine particle flotation. *Miner. Eng.* **2010**, *23*, 420–437. [CrossRef]

16.	Dai, Z.; Fornasiero, D.; Ralston, J. Particle–bubble collision models—A review. *Adv. Colloid Interface Sci.* **2000**, *85*, 231–256. [CrossRef]

17.	Hornn, V.; Ito, M.; Yamazawa, R.; Shimada, H.; Tabelin, C.B.; Jeon, S.; Park, I.; Hiroyoshi, N. Kinetic Analysis for Agglomeration-Flotation of Finely Ground Chalcopyrite: Comparison of First Order Kinetic Model and Experimental Results. *Mater. Trans.* **2020**, *61*, 1940–1948. [CrossRef]

18.	Hornn, V.; Ito, M.; Shimada, H.; Tabelin, C.B.; Jeon, S.; Park, I.; Hiroyoshi, N. Agglomeration-Flotation of Finely Ground Chalcopyrite and Quartz: Effects of Agitation Strength during Agglomeration Using Emulsified Oil on Chalcopyrite. *Minerals* **2020**, *10*, 380. [CrossRef]

19.	Hornn, V.; Ito, M.; Shimada, H.; Tabelin, C.B.; Jeon, S.; Park, I.; Hiroyoshi, N. Agglomeration–Flotation of Finely Ground Chalcopyrite Using Emulsified Oil Stabilized by Emulsifiers: Implications for Porphyry Copper Ore Flotation. *Metals* **2020**, *10*, 912. [CrossRef]

20.	Bilal, M.; Park, I.; Hornn, V.; Ito, M.; Hassan, F.U.; Jeon, S.; Hiroyoshi, N. The Challenges and Prospects of Recovering Fine Copper Sulfides from Tailings Using Different Flotation Techniques: A Review. *Minerals* **2022**, *12*, 586. [CrossRef]

21.	Leistner, T.; Peuker, U.A.; Rudolph, M. How gangue particle size can affect the recovery of ultrafine and fine particles during froth flotation. *Miner. Eng.* **2017**, *109*, 1–9. [CrossRef]

22.	Bilal, M.; Ito, M.; Akishino, R.; Bu, X.; Ul Hassan, F.; Park, I.; Jeon, S.; Aikawa, K.; Hiroyoshi, N. Heterogenous carrier flotation technique for recovering finely ground chalcopyrite particles using coarse pyrite particles as a carrier. *Miner. Eng.* **2022**, *180*, 107518. [CrossRef]

23.	Nesbitt, H.W.; Muir, I.J. X-ray photoelectron spectroscopic study of a pristine pyrite surface reacted with water vapour and air. *Geochim. Cosmochim. Acta* **1994**, *58*, 4667–4679. [CrossRef]

24.	Shirley, D.A. High-Resolution X-Ray Photoemission Spectrum of the Valence Bands of Gold. *Phys. Rev. B* **1972**, *5*, 4709–4714. [CrossRef]

25.	Park, I.; Tabelin, C.B.; Seno, K.; Jeon, S.; Inano, H.; Ito, M.; Hiroyoshi, N. Carrier-microencapsulation of arsenopyrite using Al-catecholate complex: Nature of oxidation products, effects on anodic and cathodic reactions, and coating stability under simulated weathering conditions. *Heliyon* **2020**, *6*, e03189. [CrossRef] [PubMed]

26.	Aikawa, K.; Ito, M.; Kusano, A.; Jeon, S.; Park, I.; Hiroyoshi, N. Development of a Sustainable Process for Complex Sulfide Ores Containing Anglesite: Effect of Anglesite on Sphalerite Floatability, Enhanced Depression of Sphalerite by Extracting Anglesite, and Recovery of Extracted Pb2+ as Zero-Valent Pb by Cementation Using Zero-Valent Fe. *Minerals* **2022**, *12*, 723. [CrossRef]

27.	Elizondo-Álvarez, M.A.; Uribe-Salas, A.; Bello-Teodoro, S. Chemical stability of xanthates, dithiophosphinates and hydroxamic acids in aqueous solutions and their environmental implications. *Ecotoxicol. Environ. Saf.* **2021**, *207*, 111509. [CrossRef]

28.	Zhuge, F.; Li, X.; Gao, X.; Gan, X.; Zhou, F. Synthesis of stable amorphous Cu2S thin film by successive ion layer adsorption and reaction method. *Mater. Lett.* **2009**, *63*, 652–654. [CrossRef]

29.	Biesinger, M.C.; Lau, L.W.M.; Gerson, A.R.; Smart, R.S.C. Resolving surface chemical states in XPS analysis of first row transition metals, oxides and hydroxides: Sc, Ti, V, Cu and Zn. *Appl. Surf. Sci.* **2010**, *257*, 887–898. [CrossRef]

30.	Aikawa, K.; Ito, M.; Kusano, A.; Park, I.; Oki, T.; Takahashi, T.; Furuya, H.; Hiroyoshi, N. Flotation of Seafloor Massive Sulfide Ores: Combination of Surface Cleaning and Deactivation of Lead-Activated Sphalerite to Improve the Separation Efficiency of Chalcopyrite and Sphalerite. *Metals* **2021**, *11*, 253. [CrossRef]

31.	Park, I.; Hong, S.; Jeon, S.; Ito, M.; Hiroyoshi, N. Flotation Separation of Chalcopyrite and Molybdenite Assisted by Microencapsulation Using Ferrous and Phosphate Ions: Part I. Selective Coating Formation. *Metals* **2020**, *10*, 1667. [CrossRef]

32.	Park, I.; Hong, S.; Jeon, S.; Ito, M.; Hiroyoshi, N. Flotation Separation of Chalcopyrite and Molybdenite Assisted by Microencapsulation Using Ferrous and Phosphate Ions: Part II. Flotation. *Metals* **2021**, *11*, 439. [CrossRef]

33. Yang, B.; Tong, X.; Deng, Z.; Lv, X. The Adsorption of Cu Species onto Pyrite Surface and Its Effect on Pyrite Flotation. *J. Chem.* **2016**, *2016*, 4627929. [CrossRef]

34. Eensalu, J.S.; Tõnsuaadu, K.; Adamson, J.; Oja Acik, I.; Krunks, M. Thermal decomposition of tris(O-ethyldithiocarbonato)-antimony(III)—A single-source precursor for antimony sulfide thin films. *J. Therm. Anal. Calorim.* **2022**, *147*, 4899–4913. [CrossRef]

35. Leppinen, J.O. FTIR and flotation investigation of the adsorption of ethyl xanthate on activated and non-activated sulfide minerals. *Int. J. Miner. Process.* **1990**, *30*, 245–263. [CrossRef]

36. Leppinen, J.O.; Basilio, C.I.; Yoon, R.H. In-situ FTIR study of ethyl xanthate adsorption on sulfide minerals under conditions of controlled potential. *Int. J. Miner. Process.* **1989**, *26*, 259–274. [CrossRef]